NACA RM L52B13

NACA

RESEARCH MEMORANDUM

EFFECTS OF SOME PRIMARY VARIABLES OF RECTANGULAR VORTEX GENERATORS ON THE STATIC-PRESSURE RISE THROUGH A SHORT DIFFUSER

By E. Floyd Valentine and Raymond B. Carroll

Langley Aeronautical Laboratory
Langley Field, Va.

NATIONAL ADVISORY COMMITTEE
FOR AERONAUTICS
WASHINGTON

May 22, 1952
Declassified October 12, 1954

NATIONAL ADVISORY COMMITTEE FOR AERONAUTICS

RESEARCH MEMORANDUM

EFFECTS OF SOME PRIMARY VARIABLES OF RECTANGULAR VORTEX GENERATORS ON THE STATIC-PRESSURE RISE THROUGH A SHORT DIFFUSER

By E. Floyd Valentine and Raymond B. Carroll

SUMMARY

An investigation was made of a 2:1 area ratio conical diffuser of length equal to the inlet diameter with separate variation of several basic parameters for simple nontwisted counterrotating rectangular vortex generators over a considerable range of inlet-boundary-layer thickness. The maximum values of static-pressure rise were determined for angle of attack, spacing, aspect ratio, and span-to-inlet boundary-layer thickness. Over the range of inlet-boundary-layer thickness it was shown that an increase in static-pressure rise of 40 percent could be obtained.

INTRODUCTION

In the design of aircraft internal-flow systems, the problem of providing an effective diffuser conforming to severe space limitations is frequently encountered. As part of a general consideration of this problem references 1 to 5 give recent information on the mechanism of the diffusion process and its relation to the boundary-layer characteristics for 2:1 area ratio diffusers of length equal to the inlet diameter and of length equal to about two inlet diameters.

In the case of the longer diffuser of reference 1 the flow rate was carried up to the choking value at a Reynolds number of 7.45×10^6 based on inlet diameter. For this same diffuser geometry but in reduced size and Reynolds number (reference 2), sufficient power was applied to give supersonic flow up to a Mach number of about 1.5, just short of one-half inlet diameter into the diffuser. Reference 3 gives the results obtained where the inlet transition radius was varied between zero and a radius equal to four inlet diameters.

Work with the short diffuser (references 4 and 5) has resulted in information on the effect of inlet-boundary-layer thickness and the effect of surface roughness on short-diffuser performance.

As a result of the current need for effective short diffusers in the combination of turbojet and afterburner, research has been proposed on several boundary-layer-control methods including suction, blowing, and the use of vortex generators. Vortex generators had been shown in reference 6 to be effective in reducing the power requirement of a large wind tunnel. Reference 7 gives the results obtained in a short annular diffuser with vortex generators.

The short diffuser of reference 4 had extensive separated regions for the thicker of the two values of inlet boundary layer. The static pressure rise was considered low and there was considerable flow fluctuation. Reference 8 gives the result of application of several different vortex-generator arrangements. Although the only variables considered were number, angle of attack, and longitudinal location, a 30-percent increase in static-pressure rise was obtained and the former large flow fluctuations were eliminated. The present investigation was undertaken to include separate variation of several variables and to determine whether the resultant peak values could be used to define an effective vortex-generator arrangement for values within a range of inlet-boundary-layer conditions. The vortex-generator variables considered included those of reference 8 plus aspect ratio, span-to-inlet-boundary-layer displacement thickness ratio, and ratio of the inlet-boundary-layer displacement thickness to the inlet diameter. The flow conditions ranged up to an inlet Reynolds number of 5.5×10^6 based on inlet diameter with the corresponding inlet Mach number of 0.56.

SYMBOLS

p	static pressure
H	total pressure
u	local velocity within boundary layer
U	local velocity at edge of boundary layer
y	perpendicular distance from wall, inches
δ	boundary-layer thickness at $u = U$, inches

δ^* three-dimensional boundary-layer displacement thickness, inches $\left(\int_0^\delta \left(1 - \frac{u}{U}\right)\left(1 - \frac{2y}{d}\right)dy\right)$

q_c impact pressure $(H - p)$

Δp wall static-pressure rise

l length of inlet tube

x distance upstream of inlet vortex-generator station

d tube diameter, inches

b spanwise dimension of vortex generator

c chord of vortex generator

s middle arc length between 0.3-chord stations of vortex generators

n number of vortex generators

Nondimensional vortex-generator parameters:

α angle of attack

b/c aspect ratio

δ^*_1/d_1 inlet-displacement boundary-layer-thickness parameter

x/d_1 longitudinal-location parameter

b/δ^*_1 span to inlet-boundary-layer displacement thickness

s/b spacing

A bar over a symbol indicates an average value.

Subscripts:

0 reference conditions

1 diffuser inlet condition

6 diffuser exit conditions

7 tail-pipe exit conditions

APPARATUS AND METHODS

General arrangement.- The apparatus for this investigation (fig. 1) was that used for the investigation of reference 8 except that the inlet tube length was varied and vortex generators of several other proportions and sizes were constructed. The setup consisted of a 23° conical diffuser joined to a 21-inch-diameter cylindrical entrance section by a transition shape which, in axial section, is an arc of $5\frac{3}{16}$-inch radius tangent to both the cylindrical and the conical parts. The cylindrical entrance section was preceded by an entrance bell which provided the reduction from the 54-inch ducting leading from the blower. A $1\frac{1}{2}$-inch strip of cork crumbs was glued in the small end of the entrance bell to fix the point at which transition to turbulent flow would take place. A screen of a total-pressure drop of 1.24 times the dynamic pressure was installed 5 feet upstream of the entrance bell. The crumbs were of a size that would go through an 8-mesh screen but be stopped by a 14-mesh screen. Different lengths of cylindrical entrance section were used to give a variation in inlet-boundary-layer thickness. As in reference 4, a tail pipe, $3\frac{1}{2}$ inlet diameters in length, was in place downstream of the diffuser. A photograph of the duct arrangement is shown in figure 2.

Vortex-generator arrangements.- All vortex-generator arrangements were counterrotating in accordance with the recommendations of references 6 and 8. The vortex generators were rectangular airfoils of NACA 0012 sections and could be set at any angle of attack. The extremities were not refitted for changes in angle of attack which in some cases resulted in a slight gap between the airfoil and the duct surface. At an angle of attack of 15° this gap was no more than 0.8 percent of the chord for any of the vortex generators. No attempt was made to seal this gap.

A basic arrangement from reference 8 which had 22 counterrotating vortex generators set 15° with $\frac{s}{b} = 2.85$, $\frac{b}{c} = 0.5$, $\frac{x}{d_1} = 0$, and which for these tests gave $\frac{b}{\delta^*_1} = 7.3$ and $\frac{\delta^*}{d_1} = 0.0065$ was taken as an anchor point. The general procedure was to provide for separate variation of

each parameter to include the value in the basic arrangement plus two values higher and two values lower than the value for the basic arrangement. As in reference 8, variation of spacing was accomplished by varying the number of 2-inch-chord by 1-inch-span vortex generators. The numbers employed were 10, 14, 22, and 44, which were chosen even numbers to give counterrotating arrangements. To change b/δ^*_1 and keep the other parameters constant required related changes in span, chord, and number. Using the numbers already mentioned in the variation of spacing, corresponding values of span and chord were obtained and are tabulated in table I. By the use of a fixed number of airfoils of 1-inch span with the 5 chords already required, it was possible to vary the aspect ratio while maintaining the other parameters constant. It was similarly possible to vary independently the angle of attack, the span-to-inlet-boundary-layer thickness ratio, the inlet-boundary-layer thickness, and the longitudinal location with changes in spanwise length but no additional chords.

Instrumentation.- Static-pressure measurements were wall static pressures measured at six radially distributed positions at stations 1, 6, and 7 of figure 1. A single line of flush static orifices extended upstream of the diffuser inlet. Static-pressure measurements at these points and the readings from a total-pressure tube in the large duct upstream of the inlet pipe constitute the basis for the quantitative diffuser performance data of this investigation. All pressures were observed on a multitube manometer using tetrabromoethane as a fluid. A remote-control pitot-static survey tube was used to get boundary-layer profiles in the inlet tube and at stations 6 and 7. This survey device may be seen in place at station 6 in the photograph of figure 2.

Basis of comparison of vortex-generator arrangements.- In this work, as in reference 8, a quick method of evaluating each of a number of vortex-generator arrangements was required. Reasons for the adoption of the following procedure are detailed in reference 8. Arithmetic averages of the pressures from the circumferentially distributed static-pressure orifices at station 6 and at station 7 were used for the diffuser and for the diffuser-tail-pipe exit pressure, respectively. For an inlet static pressure, use was made of a tap at least 3 chords upstream of the vortex generators in order to be out of the local pressure field of the vortex generators and also not affected by separation areas in the diffuser. These two static-pressure values were used with the upstream total-pressure reading to compute values of $\Delta p/q_{c1}$.

RESULTS AND DISCUSSION

Diffuser With No Vortex Generators

Observation of manometer board fluctuations and tufts described in reference 8 indicated that with the bare diffuser the flow fluctuated between two fairly definite patterns which were referred to as state a and state b. It appeared to be a definite alternation between two conditions rather than a simple rotation of the separated regions about the diffuser center line. In the present investigation this alternation was not so definite with the bare diffuser and it was considered that one curve could be considered representative. With some of the vortex-generator arrangements, however, there was an alternation between two definite conditions and the results of the two are presented as state a and state b in the figures. Pressure rise through the diffuser and through the diffuser plus tail pipe in terms of inlet dynamic pressure is shown in figure 3 for two inlet-velocity values as a function of δ^*_1/d_1. These are cross plots of values picked from plots of the pressure rise measured at several values of the flow rate. The values of δ^*_1 were obtained from surveys made in the inlet with the exception of that for the shortest length inlet duct which was obtained by a straight-line extrapolation of a logarithmic plot of δ^*_1/d_1 against an inlet-pipe length. This was done because the single measured value of δ^*_1/d_1 for the shortest length was so inconsistent with the other values as to indicate that it must have been influenced by some local surface condition which would prevent it from being representative of the entire inlet flow.

The pressure-rise ratio through the diffuser (fig. 3) is seen to decrease as the inlet-boundary-layer thickness increases for both inlet-velocity values. The pressure-rise ratio was lower at the higher inlet velocity. The same is true in the case of the pressure rise through the diffuser plus tail pipe except that the diminution with increase of inlet-boundary-layer thickness is not so great and there is considerably less difference between the high- and low-speed values of pressure-rise ratio. Points representing the no-vortex-generator values of reference 8 are given which are seen not to fall exactly on these curves. The reasons for this would include different boundary-layer profile because of the cork transition strip upstream of the inlet pipe, reassembly of the entire setup with new joints, and the fact that throughout the present investigation the inlet pipe just upstream of the transition section had its surface smoothness impaired by the large number of holes drilled for attaching the vortex generators. When not in use the holes were taped on the outside and filled flush with the inner surface with glazing compound. It is considered that the results with vortex generators would not be affected by these surface conditions in their immediate vicinity.

Effects of Selectable Vortex-Generator Variables

Basic condition.- The pressure recovery for the basic condition and also for an angle of attack of 22.5° are shown in figure 4 against the inlet-velocity parameter. For the 15° setting, figure 4(a), it is seen that the diffuser flow fluctuated between two values, one of which involved considerable separation effect. This is in contrast to the result of reference 8 in which this vortex-generator arrangement gave a smooth flow which could be represented by a single curve. Since the lower 15° curve was inconsistent with the results of reference 8 and also inconsistent with all the low-speed $p_1/H_0 = 0.95$ cross plots of each of the selectable vortex-generator variables about to be presented, it was considered as not representative and was ignored in these cross plots.

Angle of attack.- The effect of angle of attack is shown in figure 5. The best angle of attack for these conditions is indicated as about 20° at the low-speed and about 14° at the high-speed condition. An intermediate angle would be indicated if neither the high-speed nor the low-speed condition were to be favored.

Spacing.- In figure 6 are shown the effects of spacing. It shows clearly that unless enough vortex generators are used the flow alternates between two flow conditions, neither of which gives a high recovery. Recoveries in the case of too few vortex generators is even more reduced at the high-speed condition. There is, however, an optimum spacing of about two span lengths indicated for this condition which is the same for each of the speed conditions considered. For this optimum spacing the recovery at high speed is as great a proportion of the inlet indicated impact pressure as in the case of the low-speed condition.

Aspect ratio.- The effects of aspect ratio are shown in figure 7. It is clear that for either high or low speed the span should be no more than one-fourth the chord if steady flow with high pressure recovery is to result.

Ratio of span-to-inlet-boundary-layer displacement thickness.- In figure 8 are shown the effects of varying the span in relation to the inlet-boundary-layer displacement thickness. The best span considering both high and low speed appears to be about six times the inlet-boundary-layer displacement thickness. The ratio of span-to-inlet-boundary-layer displacement thickness does not have a predominant effect, however, for values ranging between 4 and 12.

Longitudinal location.- Figure 9 was included because it would be of interest in a case where space limitations prevented an area increase

until an appreciable length of constant-area-duct had been utilized. It indicates an advantage in this case of moving the vortex generators upstream about one-third the inlet diameter.

Effect of Inlet-Boundary-Layer Displacement Thickness

The inlet-boundary-layer displacement thickness is ordinarily a condition imposed by the particular installation being considered. The basic vortex-generator arrangement from reference 8 was applied to the diffuser for four different inlet-boundary-layer thicknesses. The results are shown in figure 10. The vortex generators gave considerable gain in static-pressure recovery in all cases for the low-speed condition. In the case of the high-speed condition, however, the gain was not so great and the flow was not as steady as evidenced by the differing values obtained in the two apparent flow conditions.

Use of the Maximum Indicated Vortex-Generator Design Values

It remains to be demonstrated whether the peak values could be used to determine vortex-generator arrangements over the range of inlet-boundary-layer displacement thickness which would be more effective than those shown in figure 10. The peak values from figures 5 to 8 supply the requirement that the spacing be about two span lengths, the aspect ratio be about one-fourth, and the span about six times the inlet-boundary-layer displacement thickness. The angle of attack to be used is not too definitely tied down but it appears that it would be in the range of 14° to 20°. With the vortex generators used in the previous part of the investigation, it was possible to approximate these values for the three largest inlet-boundary-layer thicknesses. The spacing s/b was made 2.09, and the aspect ratio was 0.327. The span in this case varied between 3.0 and 7.3 times the inlet-boundary-layer displacement thickness. However, from figure 8 the ratio of span to inlet-boundary-layer displacement thickness does not appear to be a critical quantity. Because in figure 5 the optimum angle of attack did not seem to be too clearly defined, the vortex generators were run over a range of angle of attack.

In figure 11 are shown the results of the angle-of-attack runs. From this it appears that when the peak values are used the best angle of attack is about 15° for both the high- and low-speed conditions. Figure 12 shows the variation of pressure-rise ratio with inlet pressure ratio for the three inlet-boundary-layer values. There is no decrease with increase in flow rate. The flow was quite steady. Although the two state a and state b conditions could still be discerned in some cases, the differences in the pressure rise for the two conditions were negligible. A comparison of figure 12(a) and figure 4, which are for the same span and inlet-boundary-layer displacement thickness, shows that changing the spacing and

the aspect ratio to the peak values has given an increase in the pressure-rise ratio and eliminated the difference between the pressure-rise ratios for the two apparent flow conditions.

The corresponding curves for the smallest inlet boundary layer with s/b of 2.85, b/c of 0.5, and b/δ^*_1 of 11.6 are given in figure 13. This arrangement is being considered here because, although not incorporating the optimum vortex-generator design values indicated by this investigation, it gave a pressure rise so close to the theoretical incompressible frictionless value of 0.75 times the inlet impact pressure that little further improvement could be expected. It therefore does give an indication of the maximum values to be obtained.

Figure 14 shows the effect of the vortex generators on the circumferential static-pressure distribution for an inlet-boundary-layer displacement thickness of 0.0065 of the inlet diameter. The fluctuation between two flow regimes is eliminated for the high-speed condition and at both speeds the circumferential variation is virtually eliminated.

The boundary-layer profiles at the diffuser exit usually could not be measured without vortex generators because of flow fluctuation. However, with the better vortex-generator arrangements they could be measured and did not require representation by an a and b case. Examples are given in figures 15 and 16 for four inlet-boundary-layer thicknesses. For the thickest inlet-boundary-layer displacement thickness, an approximate curve for no vortex generators could be included. The results with the vortex generators are each similar in that they indicate the velocity gradient near the wall has been increased by the vortex generators and a region of negative velocity gradient is observed.

An idea of the possibilities of simple rectangular vortex generators selected according to the material of this investigation is obtained from figure 17 which is for 30 vortex generators of aspect ratio 0.327, set 15°. The curves are extended dotted to the values at the smallest inlet boundary layer for which the vortex generators were not those indicated from figures 6 to 8, but for which the pressure recovery was nevertheless very good. It is seen that the pressure recovery for the diffuser with the selected vortex generators exceeds that of the bare diffuser by 40 percent over the entire range of inlet-boundary-layer displacement thickness and also exceeds that for the diffuser plus tail pipe for all inlet-boundary-layer displacement thicknesses up to the largest investigated at which point it is about equal to the value with diffuser plus tail pipe. Also the pressure recovery does not fall off appreciably at the high-speed condition.

SUMMARY OF RESULTS

The following statements may be made for simple rectangular non-twisted vortex generators within the range of variables investigated. The statements apply to the vortex generators when installed in a 2:1 area ratio conical diffuser of length equal to its diameter:

(1) The static-pressure rise with vortex generators selected as indicated by this investigation can be made to equal or exceed that obtained with the diffuser plus a tail pipe of $3\frac{1}{2}$ diffuser inlet diameters in length over a large range of diffuser inlet-boundary-layer thickness. This static-pressure rise is about 40 percent higher than that obtained with the diffuser alone with no vortex generators.

(2) Selection of an effective vortex-generator arrangement is not dependent on an accurate knowledge of the inlet-boundary-layer thickness.

(3) The presence of the selected vortex generators resulted in smoother and steadier flow than that of the bare diffuser for all inlet-boundary-layer displacement thicknesses.

(4) The value of pressure recovery with the selected vortex generators was maintained up to an inlet velocity for which the inlet static pressure was 0.80 of the total pressure at the center.

(5) From the static-pressure rises obtained in this investigation, it is indicated that counterrotating vortex generators in the diffuser inlet should have an aspect ratio of about one-fourth, be spaced two span lengths apart, and be set at 15° angle of attack. The span should be about six times the inlet-boundary-layer displacement thickness but might range between 4 and 10 without undue detriment.

Langley Aeronautical Laboratory
National Advisory Committee for Aeronautics
Langley Field, Va.

REFERENCES

1. Copp, Martin R., Klevatt, Paul L.: Investigation of High-Subsonic Performance Characteristics of a 12° 21-Inch Conical Diffuser, Including the Effects of Change in Inlet-Boundary-Layer Thickness. NACA RM L9H10, 1950.

2. Little, B. H., Jr., and Wilbur, Stafford W.: High-Subsonic Performance Characteristics and Boundary-Layer Investigations of a 12° 10-Inch Inlet-Diameter Conical Diffuser. NACA RM L50C02a, 1950.

3. Copp, Martin R.: Effects of Inlet Wall Contour on the Pressure Recovery of a 10° 10-Inch-Inlet-Diameter Conical Diffuser. NACA RM L51E11a, 1951.

4. Persh, Jerome: The Effect of the Inlet Mach Number and Inlet-Boundary-Layer Thickness on the Performance of a 23° Conical-Diffuser - Tail-Pipe Combination. NACA RM L9K10, 1950.

5. Persh, Jerome: The Effect of Surface Roughness on the Performance of a 23° Conical Diffuser at Subsonic Mach Numbers. NACA RM L51K09, 1951.

6. Taylor, H. D.: Application of Vortex Generator Mixing Principle to Diffusers. Concluding Report. Air Force Contract W33-038 ac-21825, U.A.C. Rep. R-15064-5, United Aircraft Corp. Res. Dept., Dec. 31, 1948.

7. Wood, Charles C.: Preliminary Investigation of the Effects of Rectangular Vortex Generators on the Performance of a Short 1.9:1 Straight-Wall Annular Diffuser. NACA RM L51G09, 1951.

8. Valentine, E. Floyd, and Carroll, Raymond B.: Effects of Several Arrangements of Rectangular Vortex Generators on the Static-Pressure Rise through a Short 2:1 Diffuser. NACA RM L50L04, 1951.

TABLE I

VORTEX-GENERATOR ARRANGEMENTS

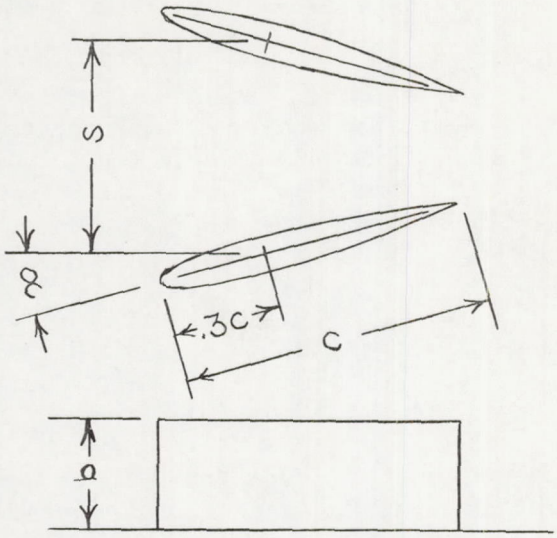

Variable	b/c	s/b	b/δ*	α	Number	Dimensions (in.)		
						c	b	s
b/c	0.240	2.85	7.3	15	22	4.16	1.00	2.85
	.327	2.85	7.3	15	22	3.06	1.00	2.85
	.500	2.85	7.3	15	22	2.00	1.00	2.85
	.673	2.85	7.3	15	22	1.48	1.00	2.85
	.977	2.85	7.3	15	22	1.02	1.00	2.85
s/b	.500	1.43	7.3	15	44	2.00	1.00	1.43
	.500	2.09	7.3	15	30	2.00	1.00	2.09
	.500	2.85	7.3	15	22	2.00	1.00	2.85
	.500	4.49	7.3	15	14	2.00	1.00	4.49
	.500	6.28	7.3	15	10	2.00	1.00	6.28
b/δ*	.500	2.85	3.7	15	44	1.02	.512	1.46
	.500	2.85	5.5	15	30	1.48	.743	2.12
	.500	2.85	7.3	15	22	2.00	1.00	2.85
	.500	2.85	11.2	15	14	3.06	1.53	4.37
	.500	2.85	15.2	15	10	4.16	2.08	5.94
α	.500	2.85	7.3	5.0	22	2.00	1.00	2.85
	.500	2.85	7.3	10.0	22	2.00	1.00	2.85
	.500	2.85	7.3	15.0	22	2.00	1.00	2.85
	.500	2.85	7.3	22.5	22	2.00	1.00	2.85
	.500	2.85	7.3	30.0	22	2.00	1.00	2.85

NACA

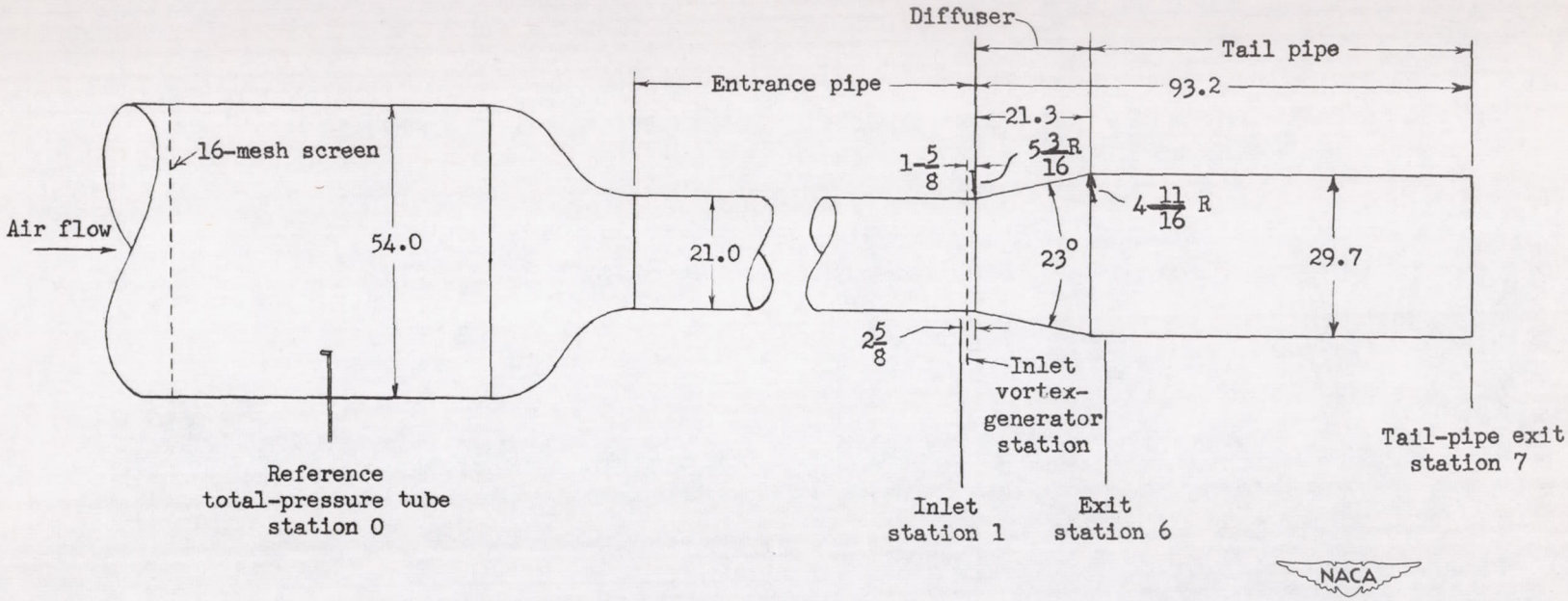

Figure 1.- General arrangement of test apparatus and instrumentation. (All dimensions are in inches.)

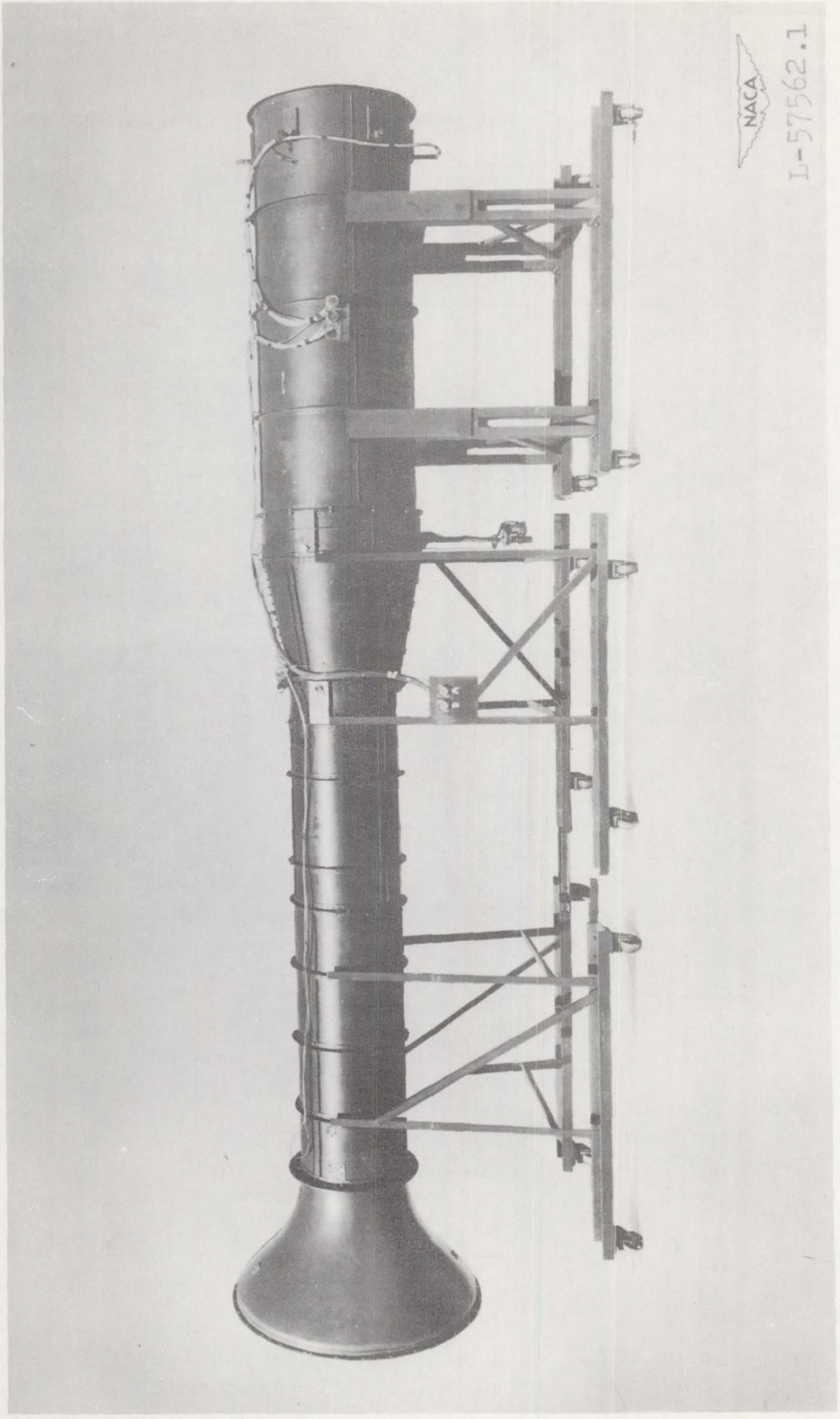

Figure 2.- General arrangement of test apparatus.

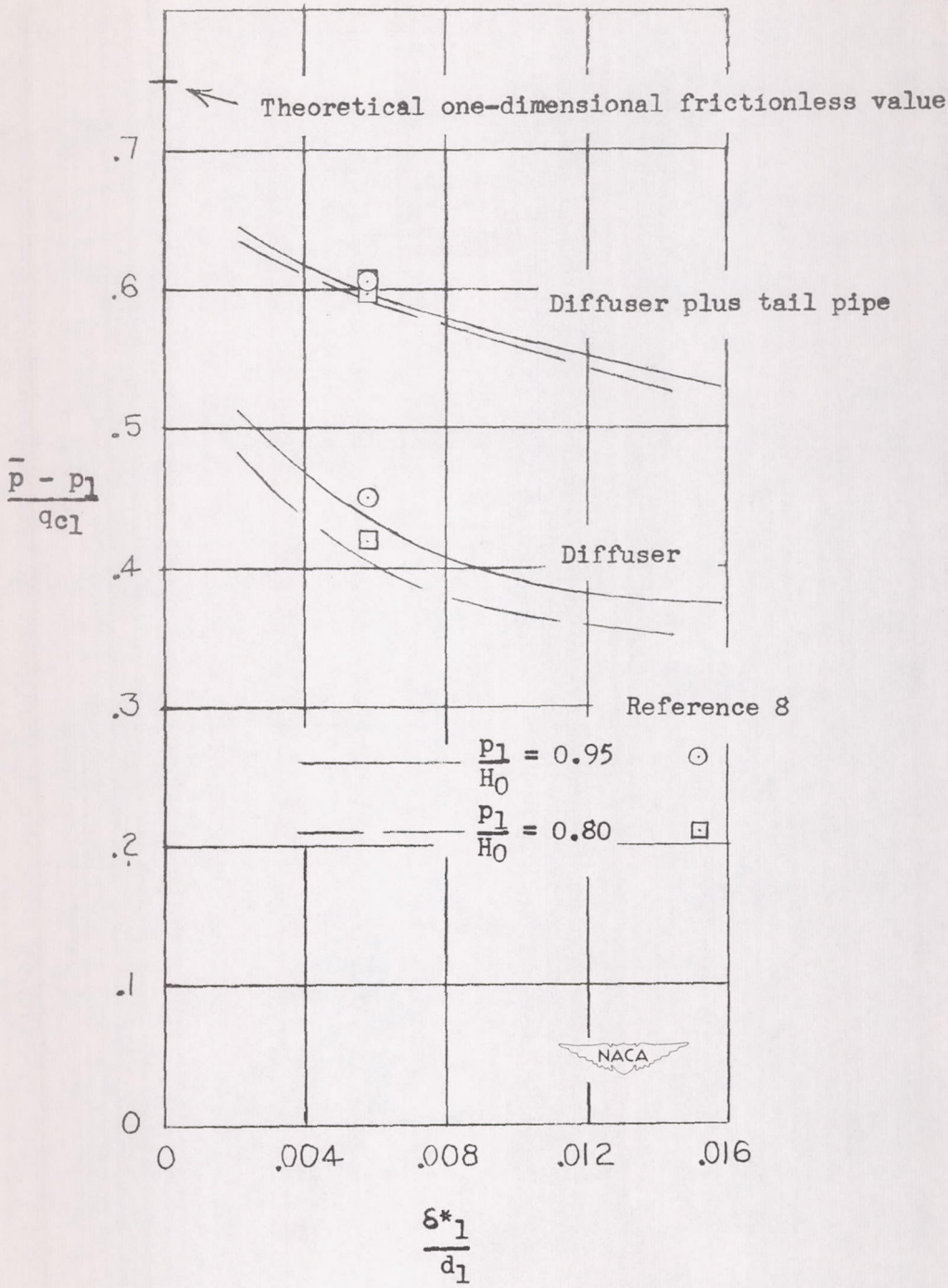

Figure 3.- Pressure-rise ratio with no vortex generators over a range of inlet-boundary-layer displacement thickness.

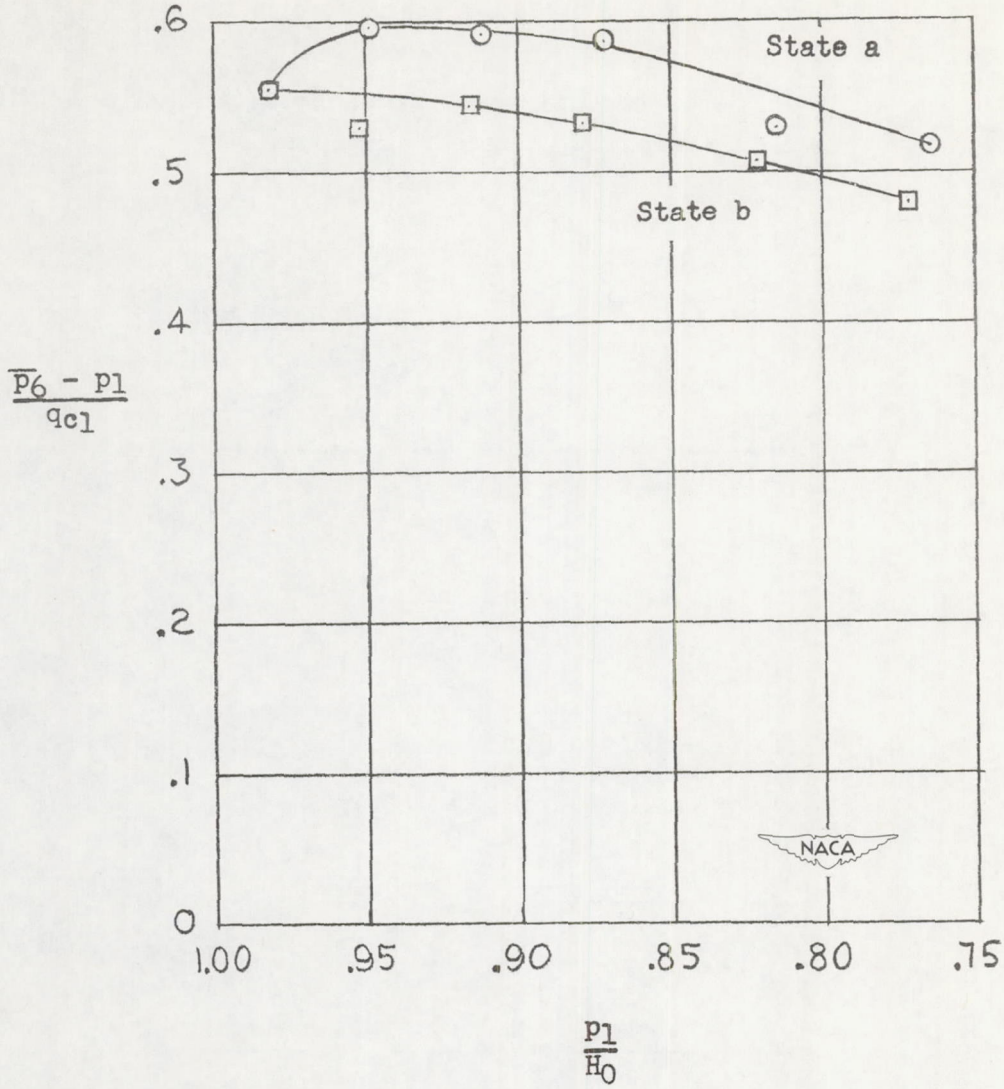

(a) $\alpha = 15^{\circ}$.

Figure 4.- Variation of pressure-rise ratio with inlet pressure ratio $\left(\frac{s}{b} = 2.85;\ \frac{b}{\delta^*_1} = 7.3;\ \frac{b}{c} = 0.5;\ \frac{\delta^*_1}{d_1} = 0.0065\right)$.

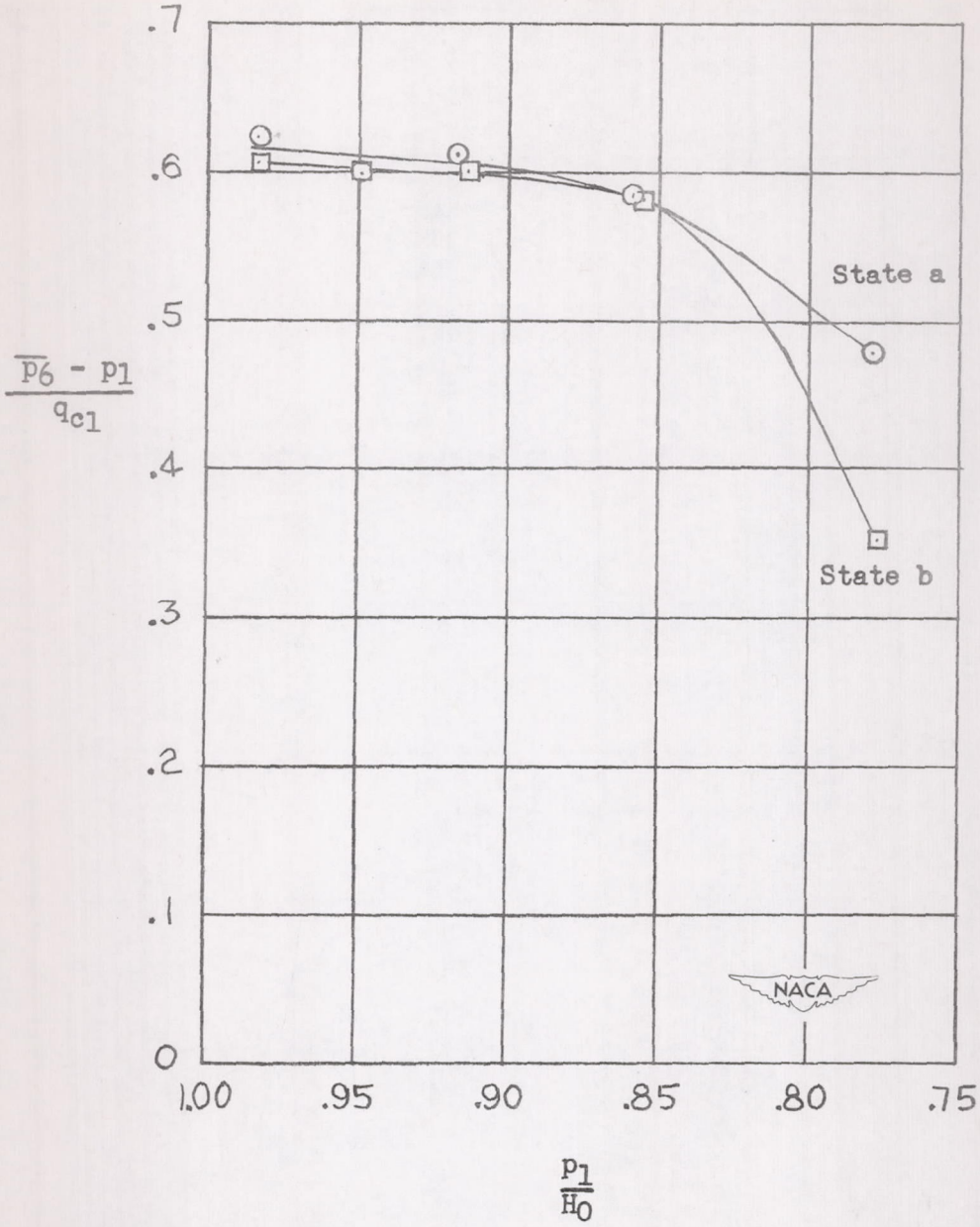

(b) $\alpha = 22.5^{\circ}$.

Figure 4.- Concluded.

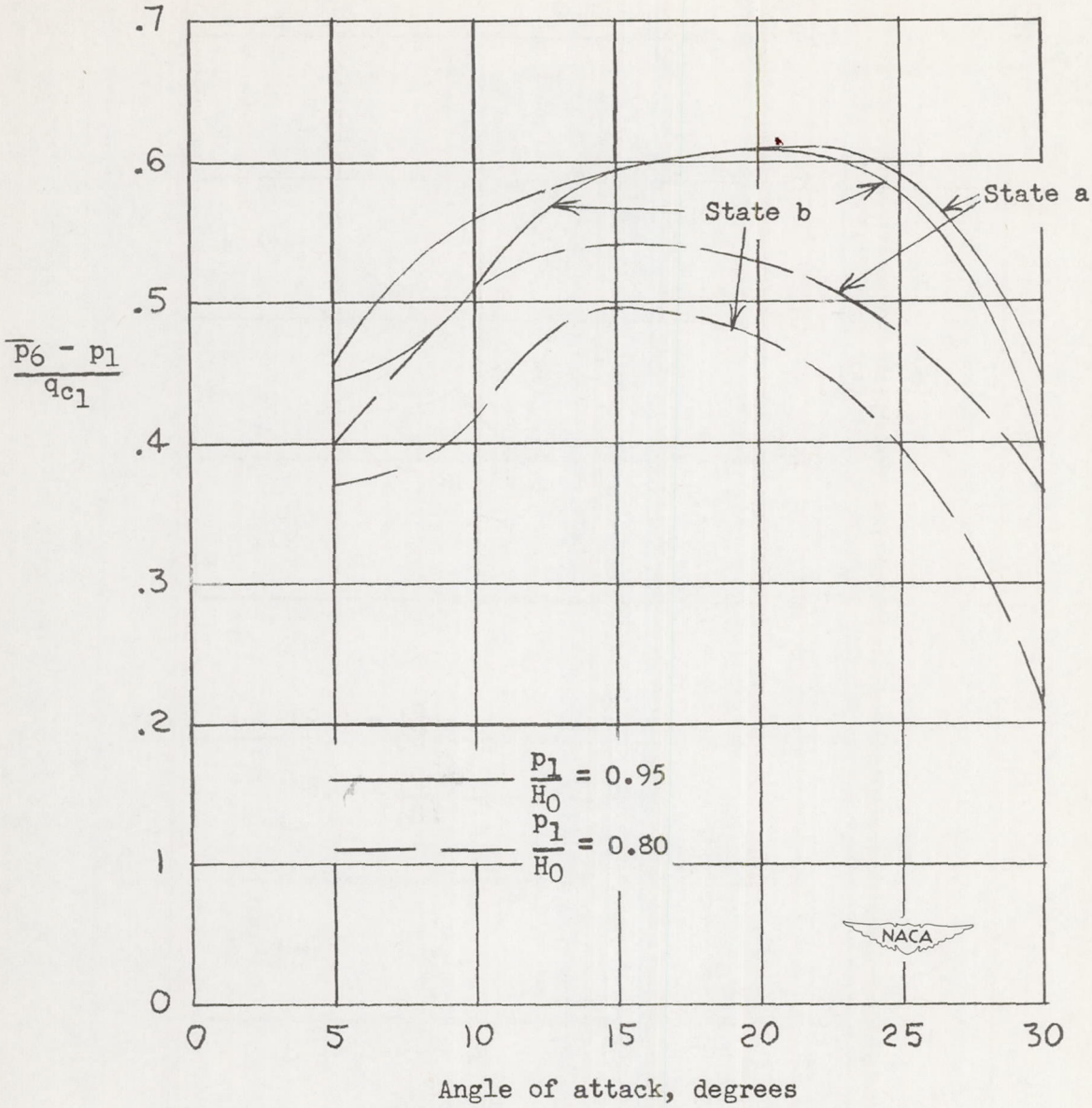

Figure 5.- Effect of vortex-generator angle of attack $\left(\frac{s}{b} = 2.85;\ \frac{b}{\delta^*_1} = 7.3;\ \frac{b}{c} = 0.5;\ \frac{\delta^*_1}{d_1} = 0.0065\right)$.

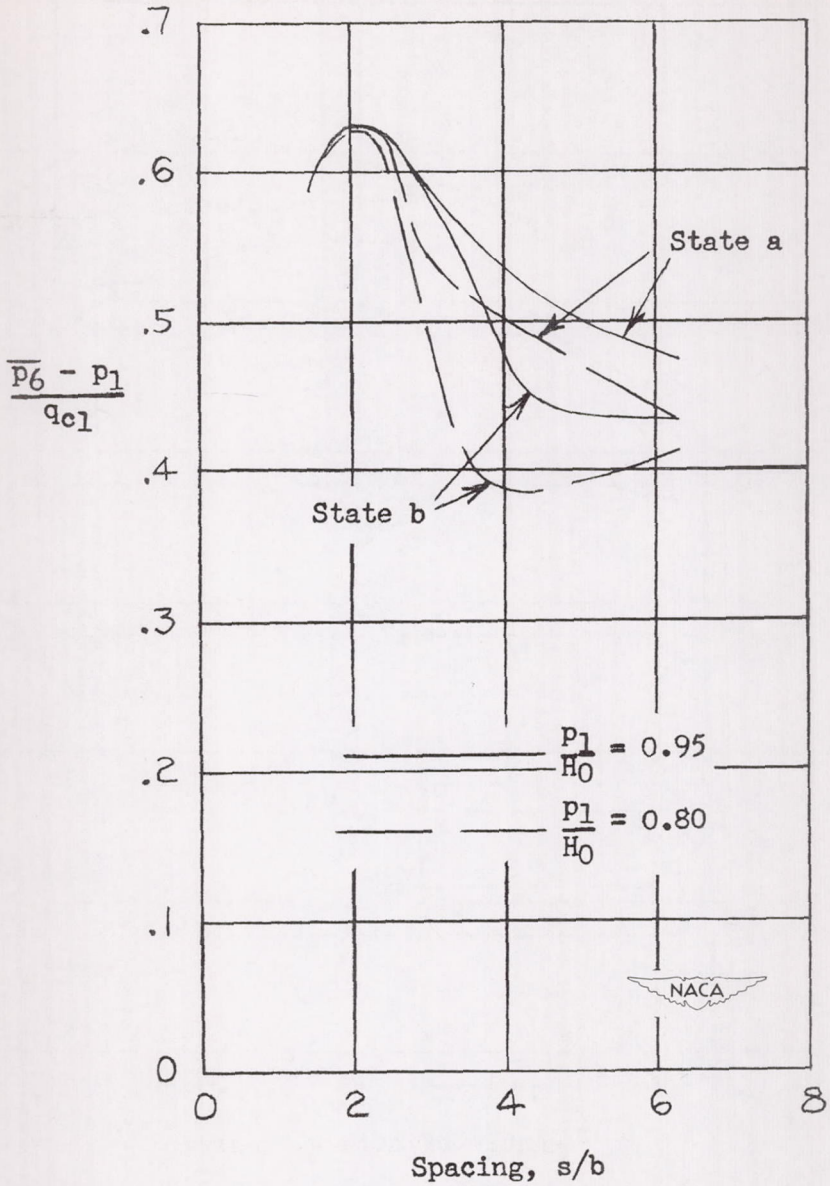

Figure 6.- Effect of vortex-generator spacing $\left(\frac{b}{\delta^*_1} = 7.3;\ \frac{b}{c} = 0.5;\ \alpha = 15^\circ;\ \frac{\delta^*_1}{d_1} = 0.0065\right)$.

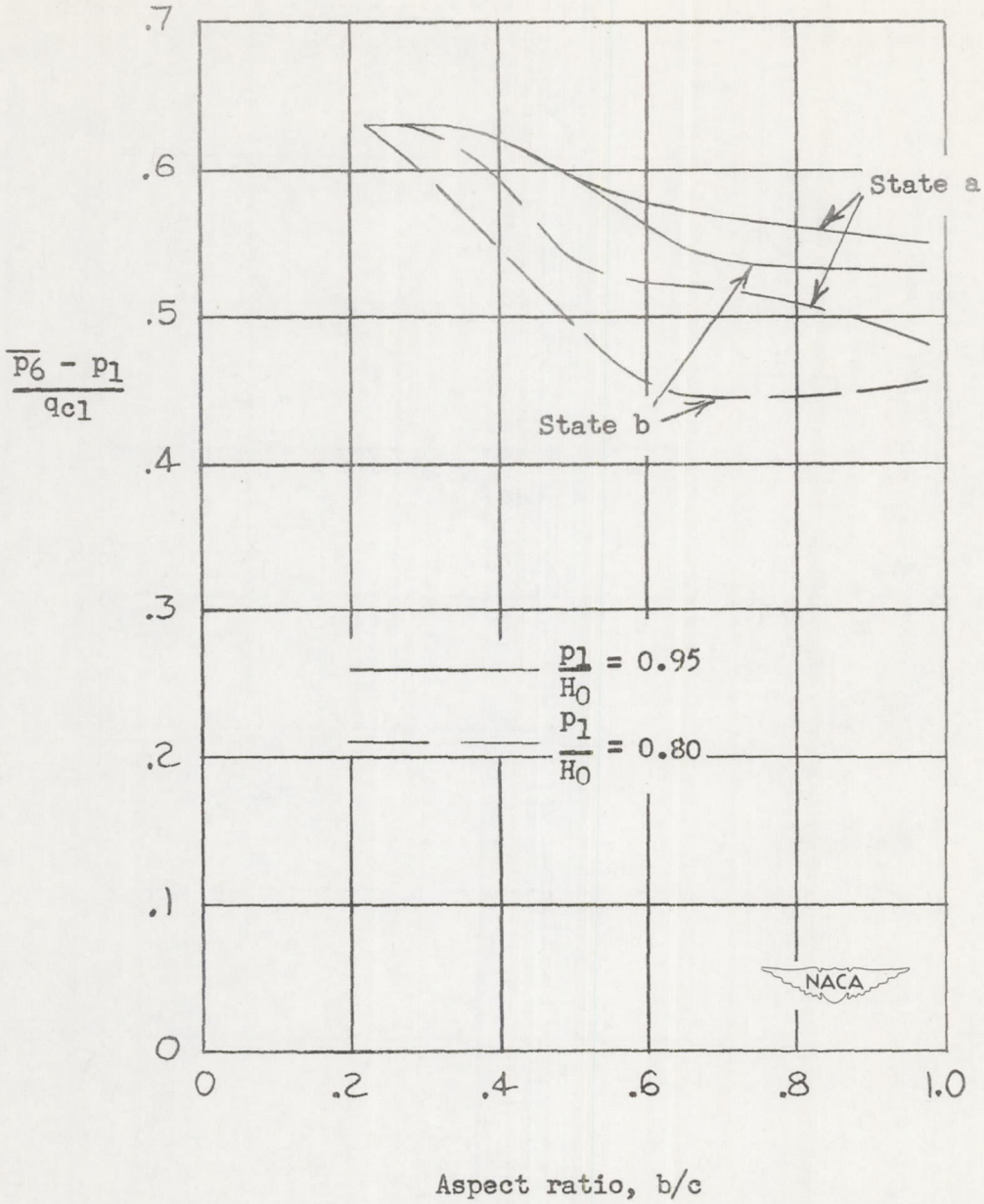

Figure 7.- Effect of vortex-generator aspect ratio $\left(\frac{s}{b} = 2.85;\ \frac{b}{\delta^*_1} = 7.3;\ \alpha = 15^\circ;\ \frac{\delta^*_1}{d_1} = 0.0065\right)$.

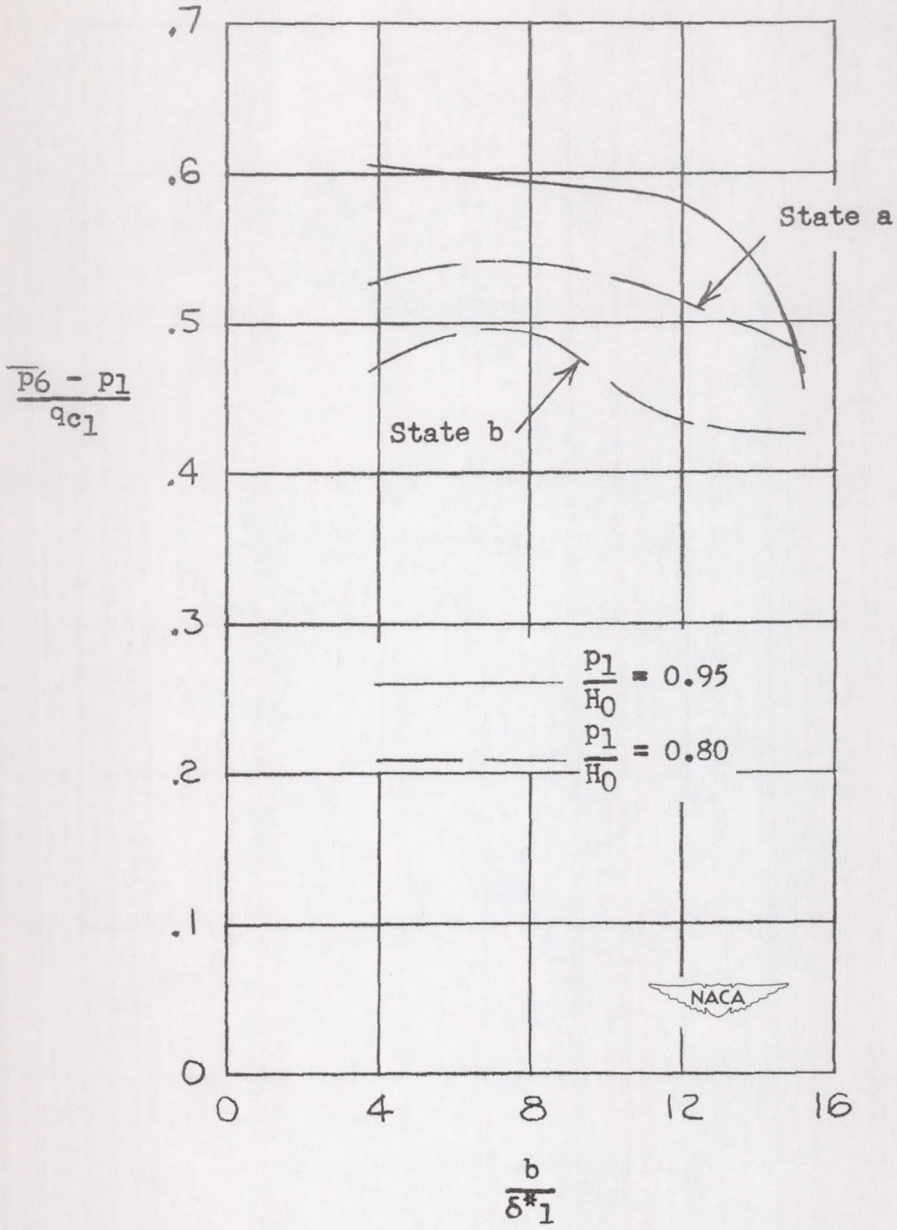

Figure 8.- Effect of vortex-generator span $\left(\frac{s}{b} = 2.85;\ \frac{b}{c} = 0.5;\ \alpha = 15^{\circ};\ \frac{\delta^*_1}{d_1} = 0.0065\right)$.

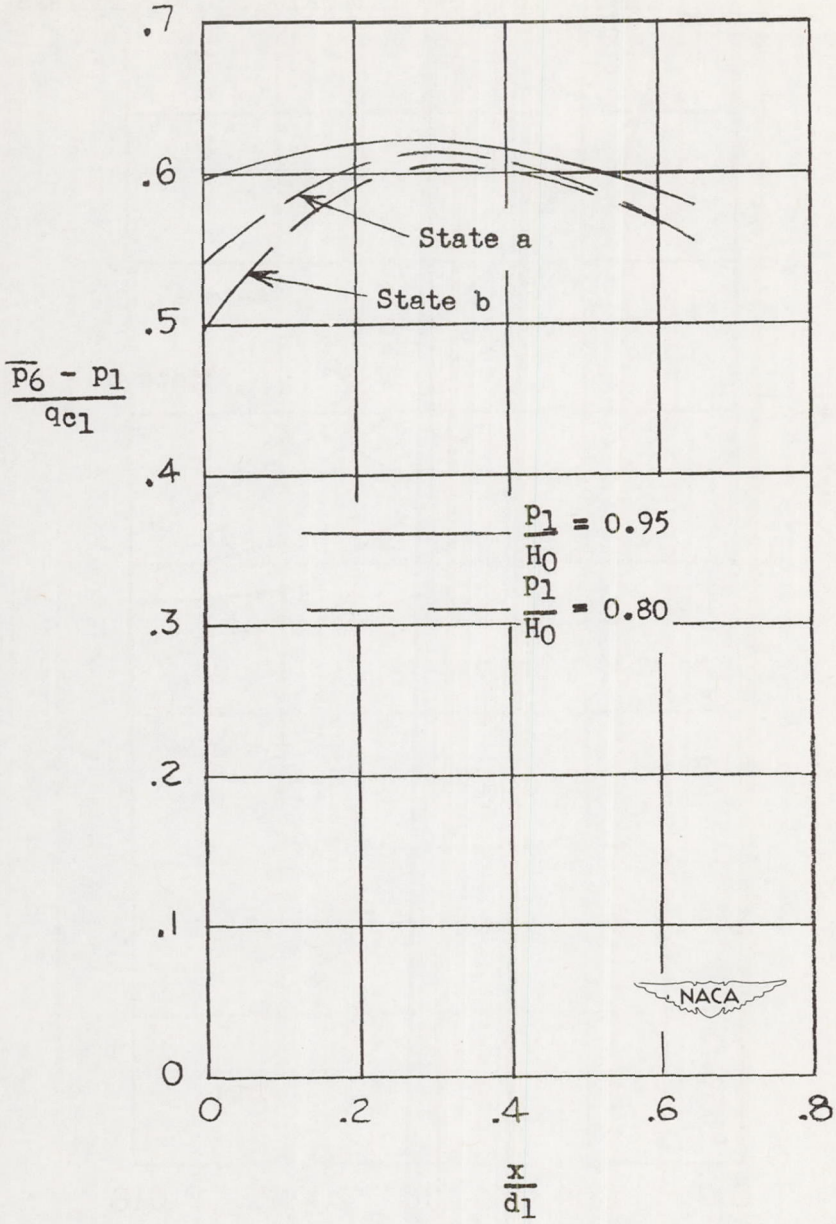

Figure 9.- Effect of moving vortex generators upstream in the inlet tube $\left(\frac{s}{b} = 2.85;\ \frac{b}{\delta^*_1} = 7.3;\ \frac{b}{c} = 0.5;\ \alpha = 15^\circ;\ \frac{\delta^*_1}{d_1} = 0.0065\right)$.

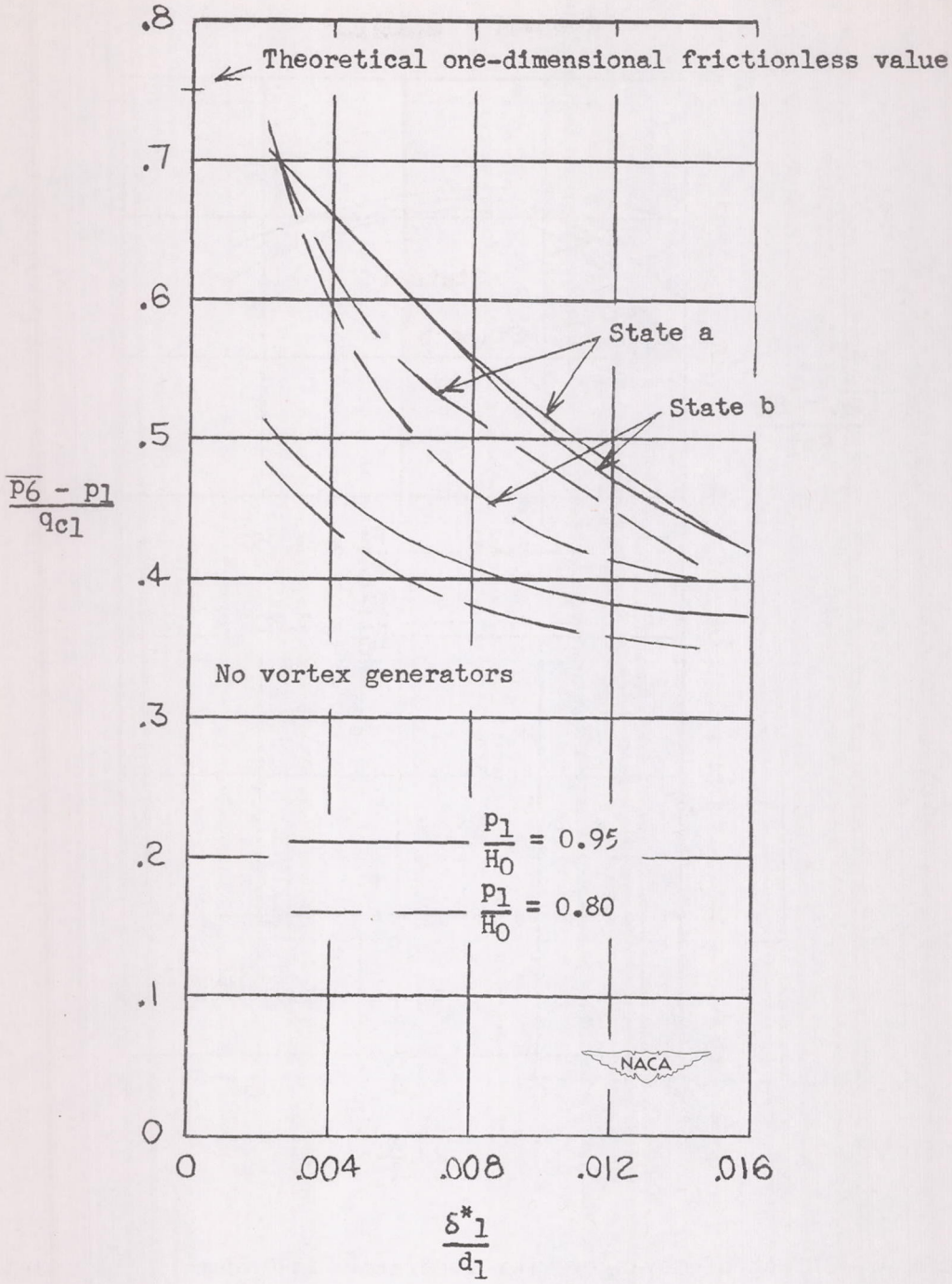

Figure 10.- Variation of pressure-rise ratio with vortex generators over a range of inlet-boundary-layer displacement thickness $\left(\frac{s}{b} = 2.85; \frac{b}{\delta^*_1} = 7.3; \frac{b}{c} = 0.5; \alpha = 15^\circ\right)$.

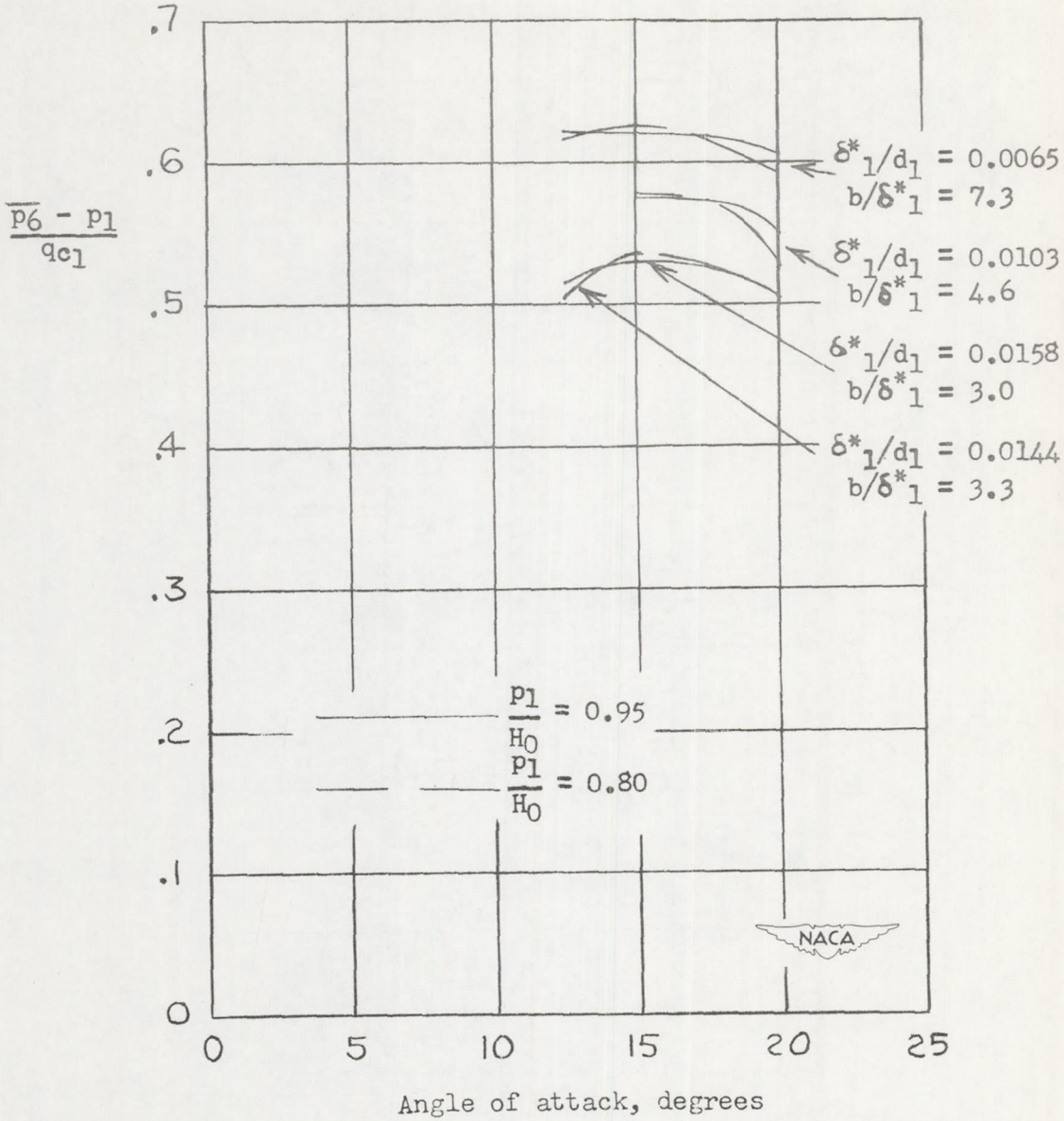

Figure 11.- Effect of vortex-generator angle of attack $\left(\frac{s}{b} = 2.09;\ \frac{b}{c} = 0.327\right)$.

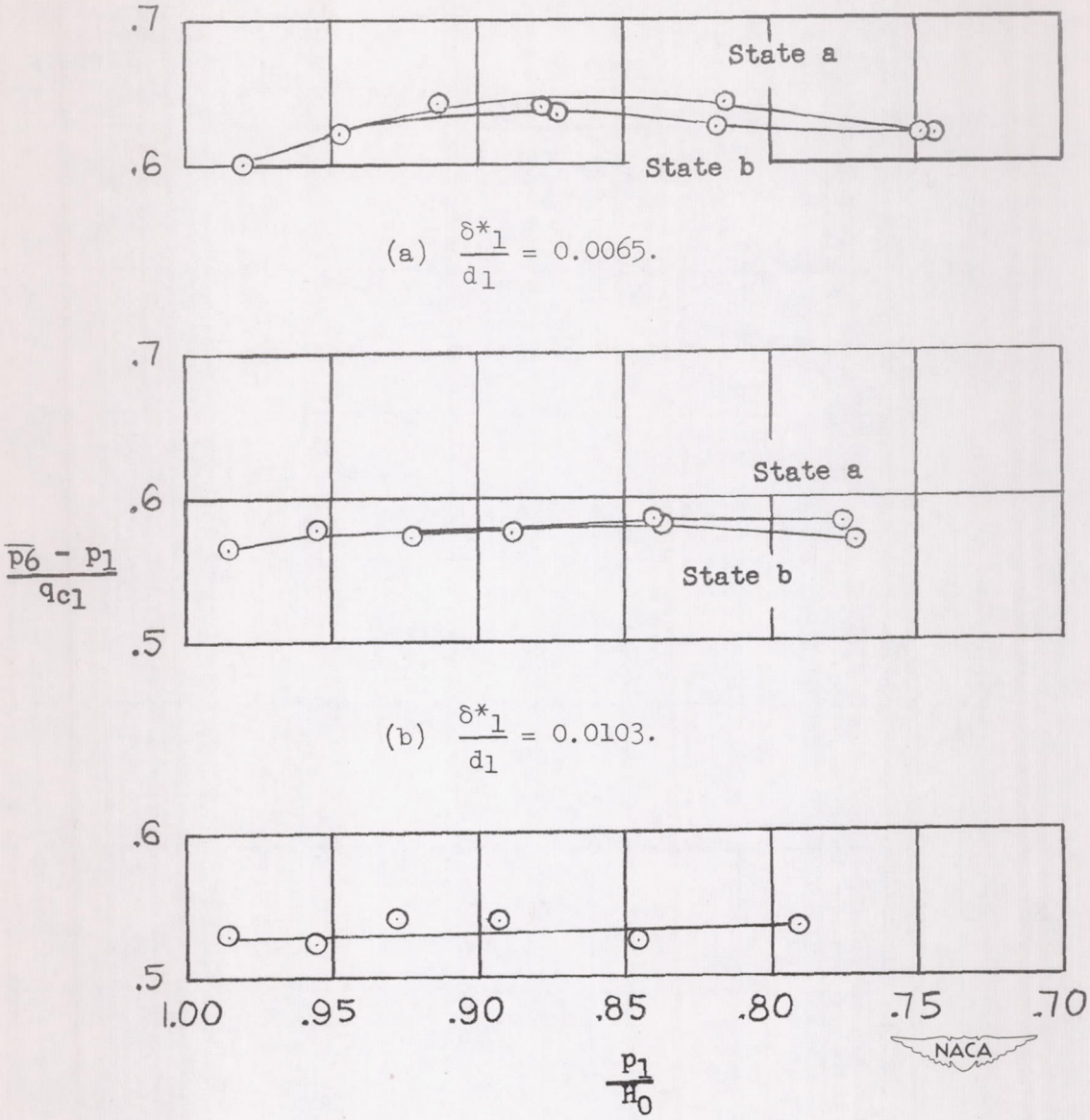

Figure 12.- Variation of pressure-rise ratio with inlet pressure ratio for three inlet-boundary-layer-displacement-thickness ratios $\left(\frac{s}{b} = 2.09;\ \frac{b}{c} = 0.327;\ \alpha = 15^{\circ}\right)$.

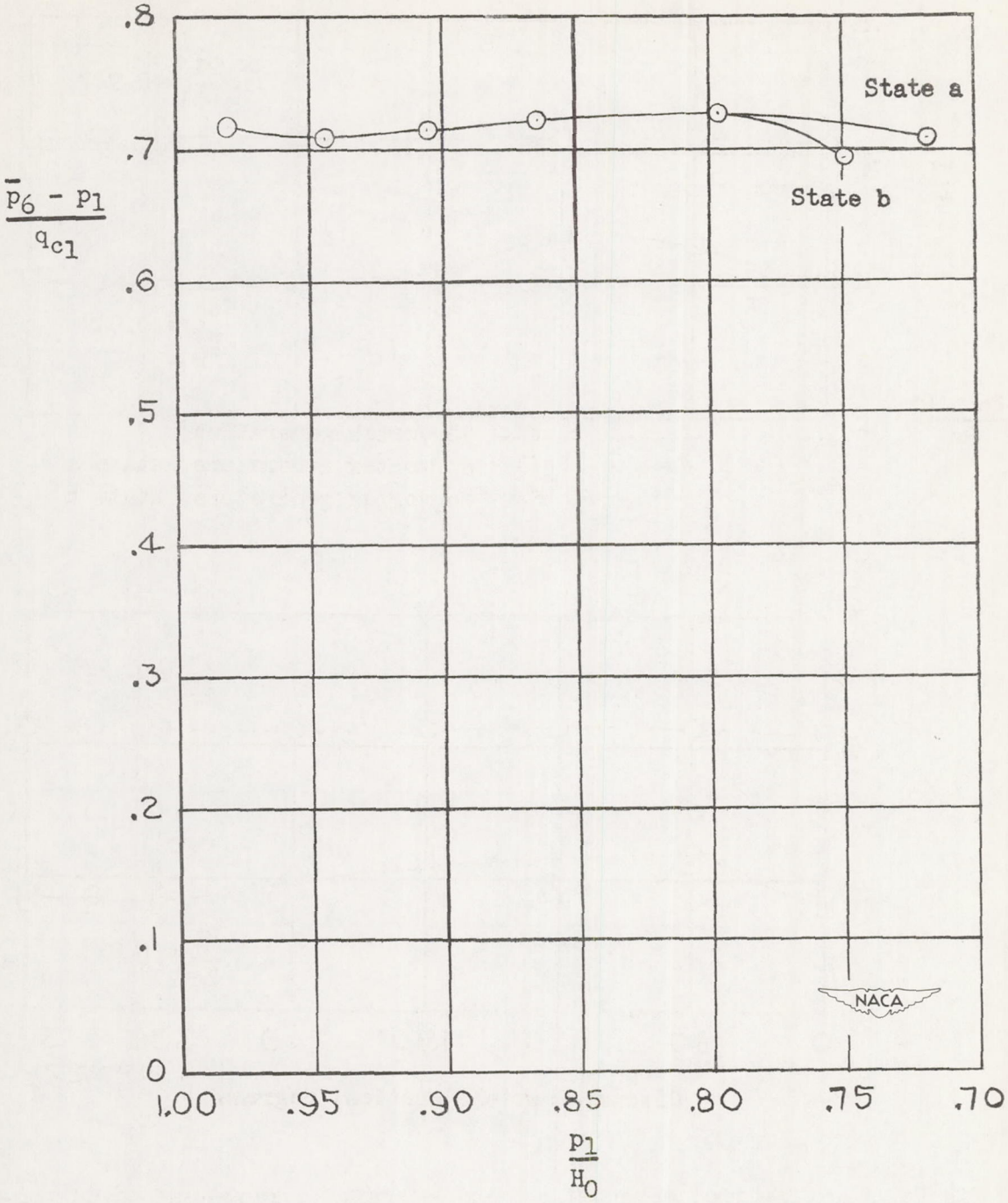

Figure 13.- Pressure-rise ratio with lowest inlet-boundary-layer-displacement thickness $\left(\frac{s}{b} = 2.85;\ \frac{b}{\delta^*_1} = 11.6;\ \frac{b}{c} = 0.5;\ \alpha = 15^\circ;\ \frac{\delta^*_1}{d_1} = 0.0021\right)$.

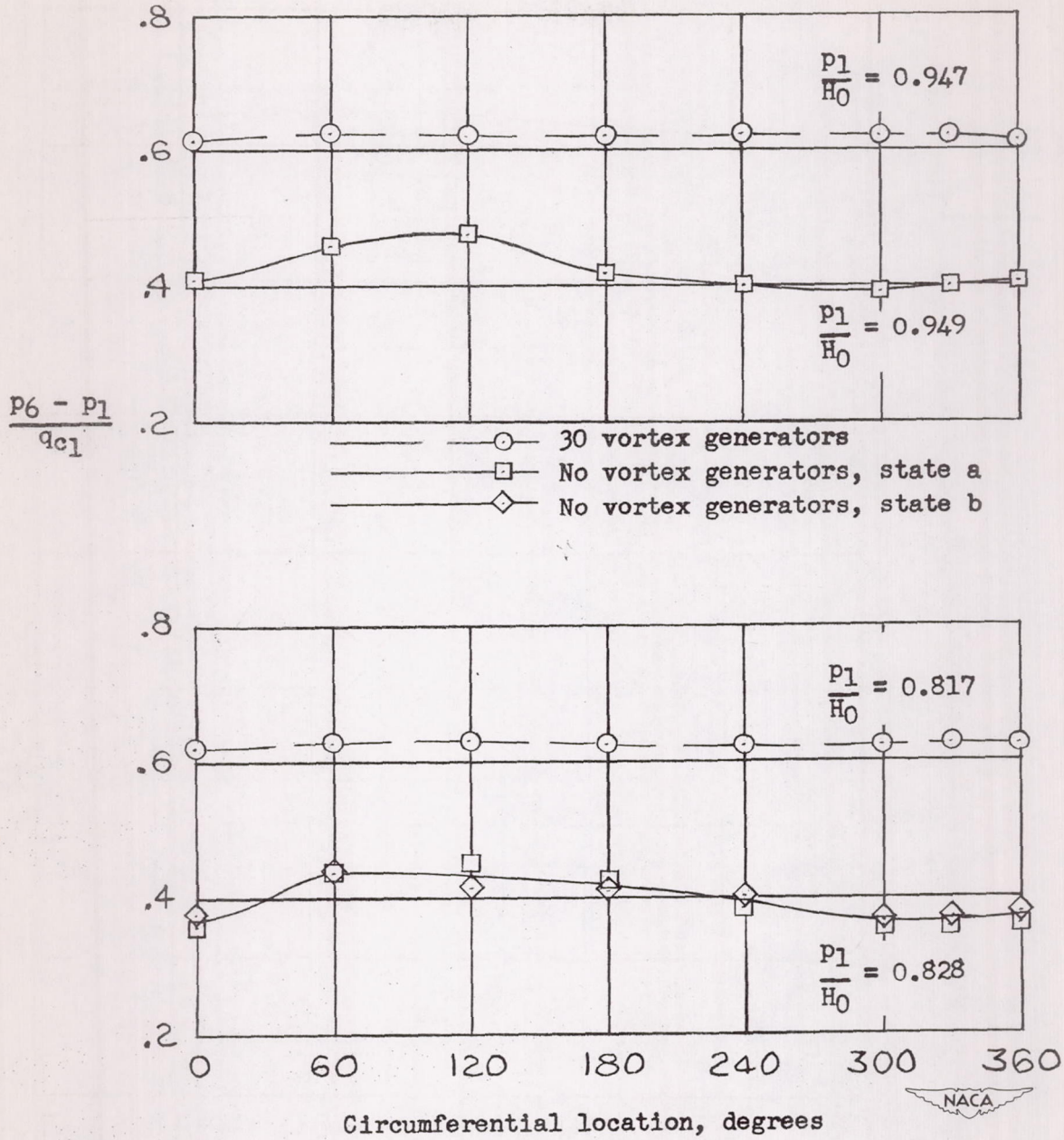

Figure 14.- Effect of selected vortex-generator arrangement on circumferential static-pressure variation at the diffuser exit $\left(\frac{s}{b} = 2.09; \frac{b}{\delta^*_1} = 7.3; \frac{b}{c} = 0.327; \alpha = 15^\circ; \frac{\delta^*_1}{d_1} = 0.0065\right)$.

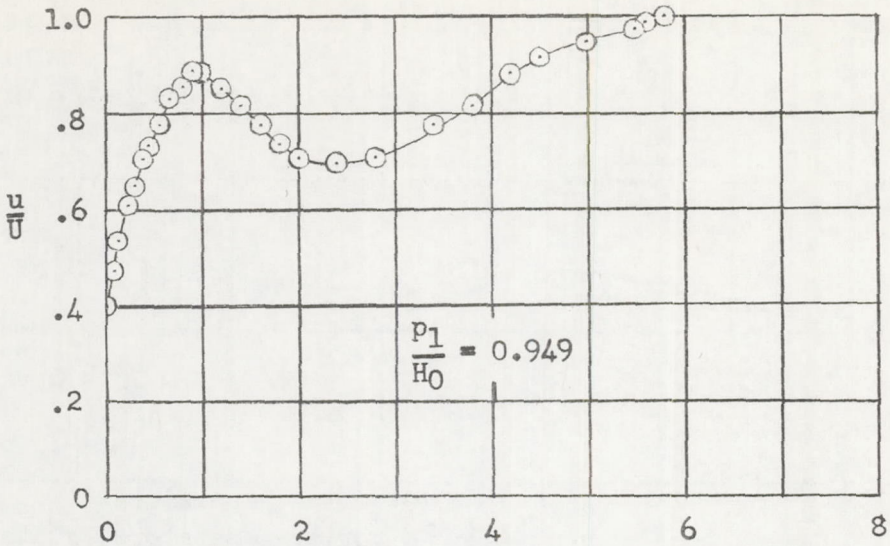

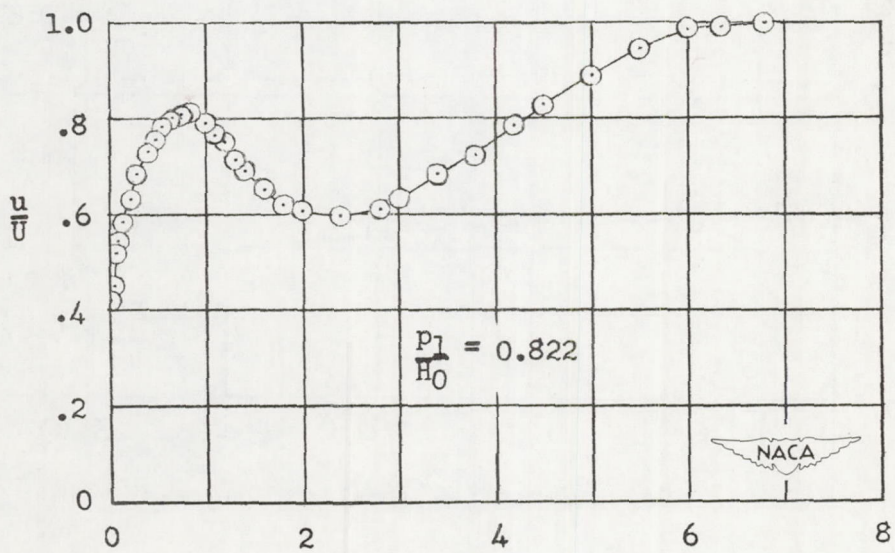

(a) $\frac{b}{\delta^*_1} = 7.3$; $\alpha = 17.5^\circ$; $\frac{\delta^*_1}{d_1} = 0.0065$.

Figure 15.- Diffuser-exit boundary-layer surveys $\left(\frac{s}{b} = 2.09;\ \frac{b}{c} = 0.327\right)$.

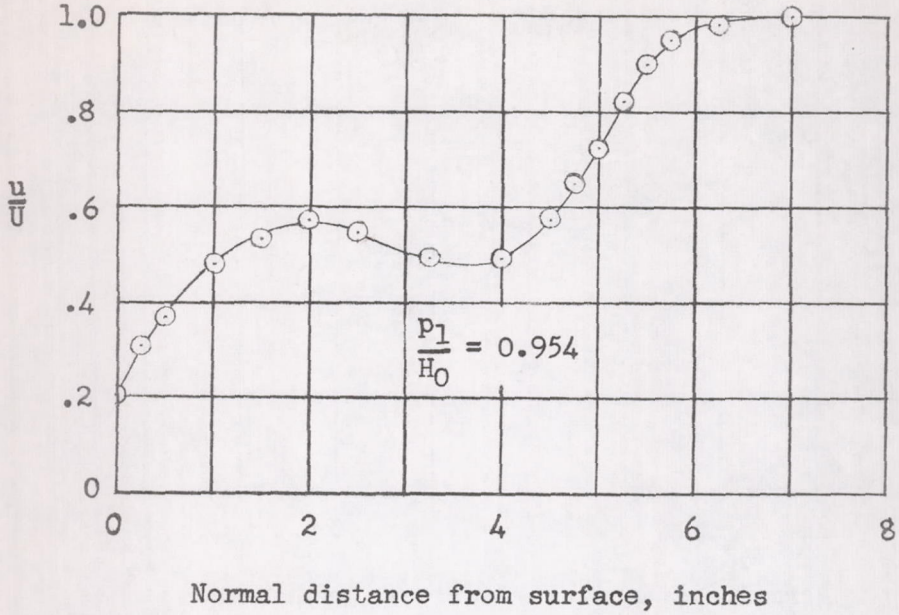

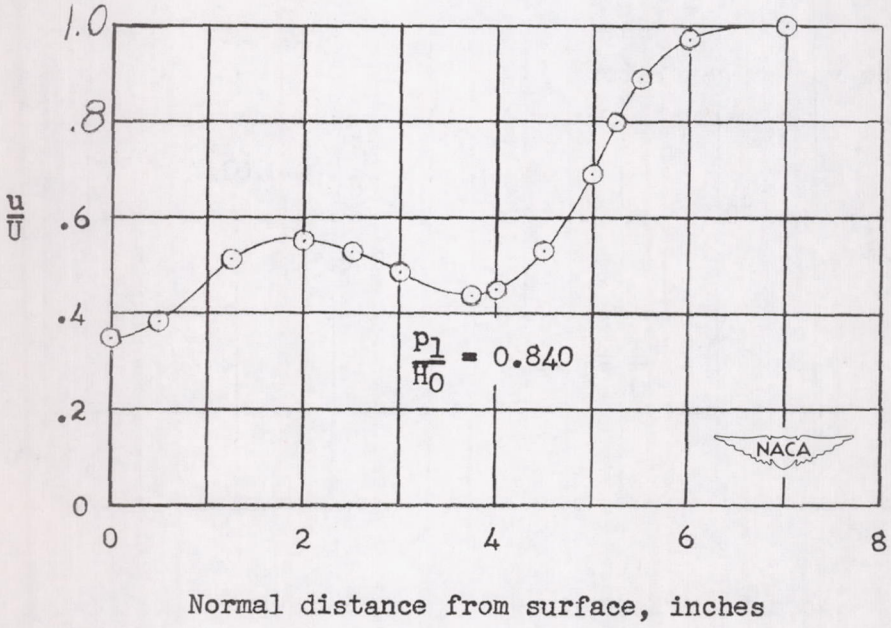

(b) $\frac{d}{\delta^*_1} = 4.6$; $\alpha = 15^\circ$; $\frac{\delta^*_1}{d_1} = 0.0103$.

Figure 15.- Continued.

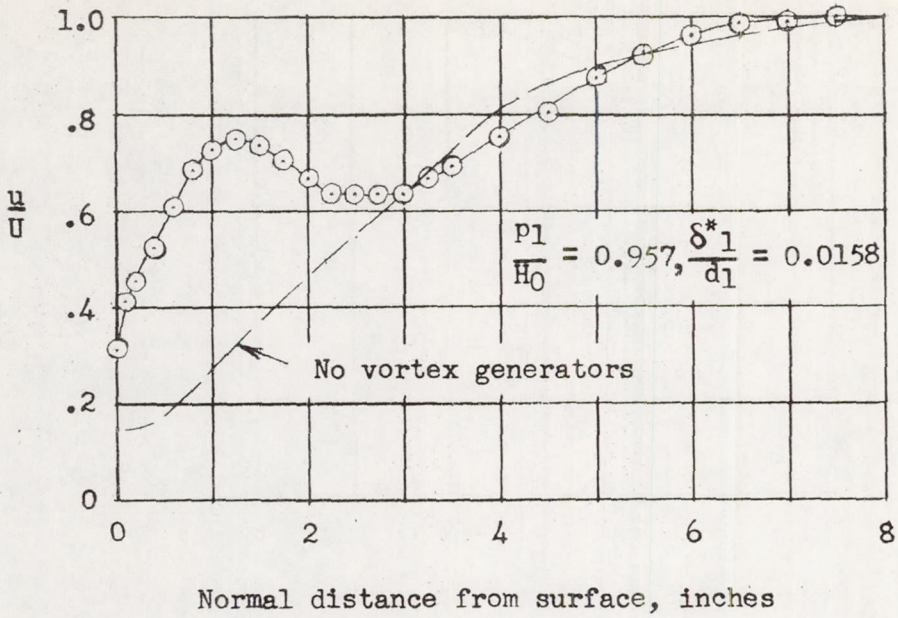

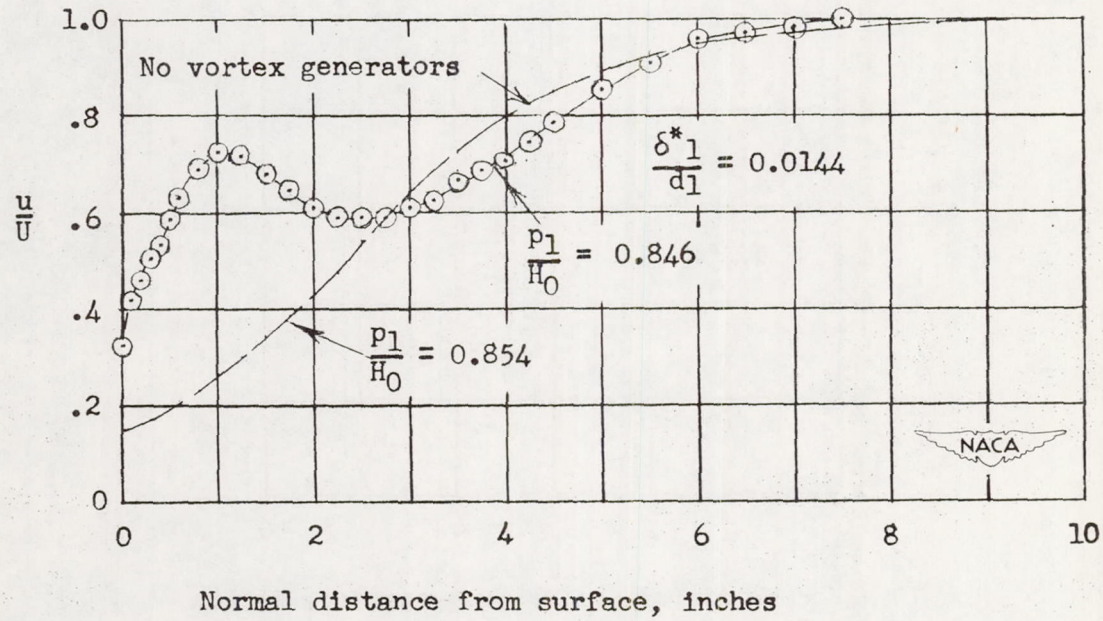

(c) $\frac{b}{\delta^*_1} = 3.0;\ \alpha = 15^\circ.$

Figure 15.- Concluded.

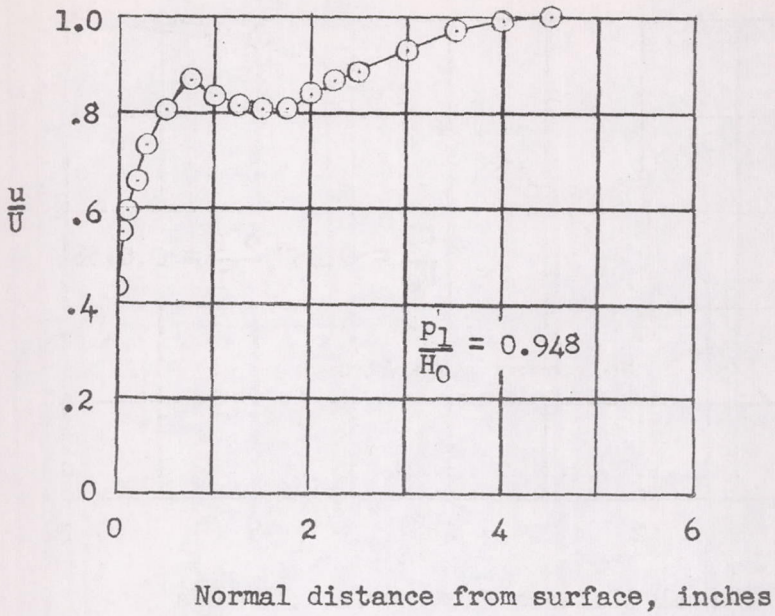

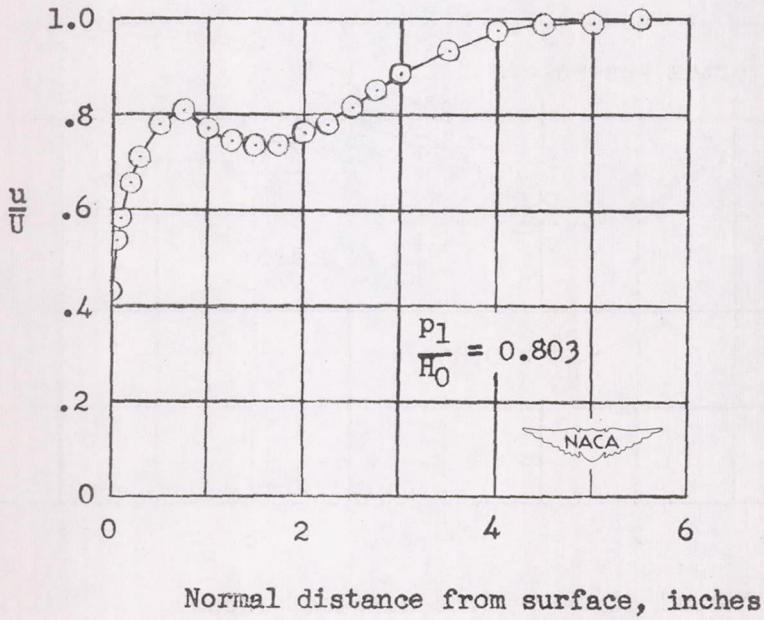

Figure 16.- Diffuser-exit boundary-layer surveys $\left(\frac{s}{b} = 2.85;\ \frac{b}{\delta^*_1} = 11.6;\ \frac{b}{c} = 0.5;\ \alpha = 15^\circ;\ \frac{\delta^*_1}{d_1} = 0.0021\right)$.

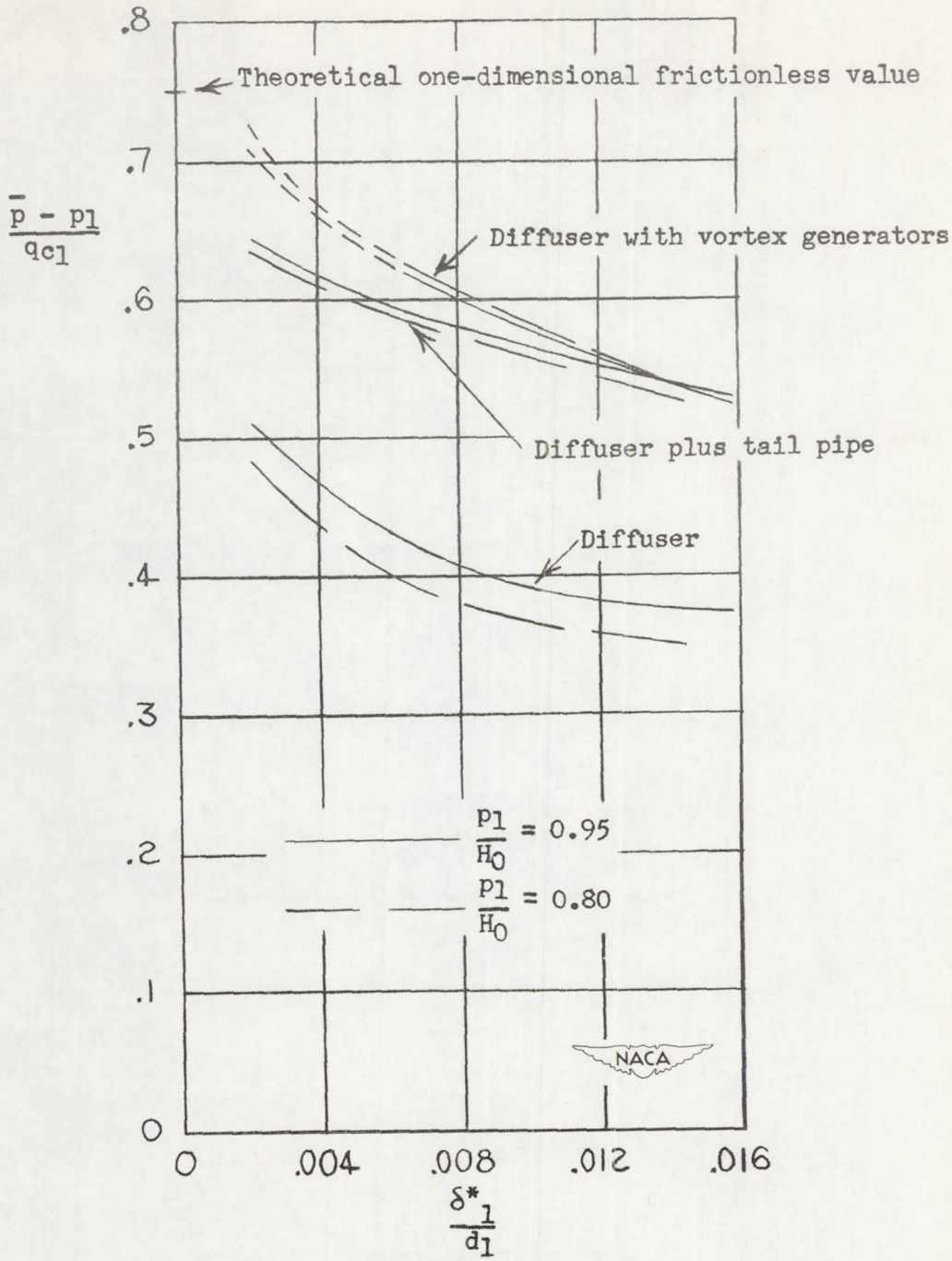

Figure 17.- Pressure-rise ratio with the selected vortex generators for a range of inlet-boundary-layer-displacement thickness $\left(\frac{s}{b} = 2.09;\ \frac{b}{c} = 0.327;\ \alpha = 15^\circ\right)$.